Path Loss Prediction in Evaporation Ducts Based on Deep Neural Network

Bingwei Shu, Wensheng Zhang, *Member, IEEE*, Yunfei Chen, *Senior Member, IEEE*, Jian Sun, *Member, IEEE*, and Cheng-Xiang Wang, *Fellow, IEEE*

***Abstract*—The evaporation duct effect is a critical issue in maritime wireless communications. This letter presents a novel scheme based on the deep neural network (DNN) for accurately predicting path loss (PL) in evaporation ducts. The environment and antenna parameters are employed as inputs for the lightweight model, enhancing its applicability to natural scenarios. The proposed scheme can achieve superior prediction performance than the k-nearest neighbor model, random forests model, and linear regression model at varying frequencies. Additionally, this letter studies the impact of the frequency, receiver height, and transmission distance on the prediction accuracy of DNN. Simulation results show that DNN exhibits high prediction accuracy at low frequencies but experiences a slight accuracy reduction at higher frequencies due to the presence of complex peak regions. The impact of receiver height and transmission distance on the prediction accuracy is not significant.**

***Index Terms*—Deep neural network, maritime wireless communication, evaporation duct, path loss, parabolic equation.**

I. Introduction

With the rapid development of wireless communications, research on the sixth generation (6G) has commenced in recent years [1]. The space-air-ground integrated network (SAGIN) has been considered an important research direction of 6G [2]. Maritime wireless communications, as an essential part of SAGIN, are increasingly prioritizing high efficiency and quality. There is also a focus on providing broadband data services over the ocean using higher bands. Maritime channel modeling is crucial to the construction of communication links. However, the complex maritime transmission environment presents various challenges, including barometric changes, sea wave movement, sparse scattering, and atmospheric duct effects [3]. The time-varying characteristics pose a significant challenge to obtain the channel response and the path loss (PL) calculation provides a practical method for evaluating signal degradation in the maritime environment, especially in the duct environment. As an important category of electromagnetic (EM) environments, atmospheric ducts are atmospheric structures with special super refraction caused by non-standard atmospheric conditions. Beyond line-of-sight (BLOS) detections and communications can be realized by atmospheric ducts [4]. Atmospheric ducts are generally divided into evaporation ducts, surface ducts, and elevated ducts. Evaporation ducts frequently appear in large areas of the sea (the probability of occurrence near the South China Sea is close to 80% [5]), and typically with heights below 40 m.

The typical methods to describe the EM propagation characteristics in atmospheric ducts include ray tracing and parabolic equation (PE). The ray tracing method employs geometric optical approximations to simulate the propagation path of high-frequency EM waves. The PE method, as an approximation of the Helmholtz equation, is widely used to calculate PL for its ability to simulate complex boundary conditions and atmospheric parameter changes. Nevertheless, these physical prediction methods have limitations in their applications due to the extended calculation time with changes in propagation range, making it difficult to meet real-time demands. Furthermore, it is difficult to quantify the dynamic changes of the required detailed reanalysis data, such as the vertical refractivity distribution of the atmosphere.

In the context of artificial intelligence has been widely used in the wireless channel prediction [6], deep learning provides a new way for PL prediction in atmospheric ducts. In [7], a feedforward neural network was constructed to predict PL at a coordinate point with an accuracy of about 90%. In [8], the PL values at different distances were regarded as a time series and predicted based on a time convolution network. In [9] and [10], different multiscale decomposition prediction methods based on the long short-term memory network were applied to enhance the prediction accuracy. In [11], a method based on the gated recurrent unit network was proposed to predict PL at different time points. However, these methods only predict one PL value per prediction action. For many scenarios, it may be necessary to obtain multiple PL values at specific heights or distances for link analysis purposes. Moreover, in practical applications, the advantages of lightweight, easy deployment, and high real-time models are significantly pronounced.

The PL in a duct environment is influenced by various factors, such as the maritime environment and antenna parameters. Treating multiple PL values as a vector introduces a complex nonlinear relationship. The deep neural network (DNN) can fit highly complex functions with the feature transformation of multiple nonlinear maps. A DNN with a few well-tuned layers can demonstrate excellent fitting ability if the width is appropriately chosen. In light of these, utilizing DNN to predict multiple PL values in evaporation ducts emerges as a straightforward, efficient, and accurate approach. The main

This work was supported by the National Natural Science Foundation of China (NSFC) under Grant 62071276, the National Key R&D Program of China under Grant 2022YFF0604903, the Natural Science Foundation of Shandong Province under Grant ZR2020MF002.

Bingwei Shu, Wensheng Zhang (Corresponding author), Jian Sun are with the Shandong Provincial Key Lab of Wireless Communication Technologies, School of Information Science and Engineering, Shandong University, Qingdao 266237, China (e-mail: bingweishu@mail.sdu.edu.cn; zhangwsh@sdu.edu.cn; sunjian@sdu.edu.cn).

Yunfei Chen is with the School of Engineering, University of Warwick, Coventry CV4 7AL, U.K. (e-mail: yunfei.chen@warwick.ac.uk).

Cheng-Xiang Wang (Corresponding author) is with the National Mobile Communications Research Laboratory, School of Information Science and Engineering, Southeast University, Nanjing, Jiangsu 210096, China, and also with the Purple Mountain Laboratories, Nanjing 211111, China (e-mail: chxwang@seu.edu.cn).

contributions of this letter can be summarized as follows:

1) A novel DNN scheme is proposed to predict multiple PL values in evaporation ducts for maritime wireless communications. Six environment parameters and three transmitting parameters are considered to enhance the models applicability to natural scenarios. The characteristics of being lightweight and enabling fast predictions ensure the practical applicability of the model.
2) The proposed DNN model can effectively and accurately predict a set of PL values for varying heights or transmission distances. The proportion of prediction results with relative errors below 5% exceeds 99%. The comparisons show that the performance of the DNN model is better than that of the k-nearest neighbors model (KNN), random forests model (RF), and linear regression model (LR).
3) Several key factors affecting prediction accuracy are studied. Simulation results indicate that the prediction accuracy is not significantly affected by the receiver height or transmission distance but slightly decreases with increasing frequency due to complex variations in the peak regions.

The rest of this letter is arranged as follows. Section II introduces related work and details the proposed DNN framework for PL prediction. Section III provides the comparison and analysis of prediction results and performance. Finally, conclusions are presented in Section IV.

II. Methods and Framework

A. Parabolic Equation Method

The PE method effectively simulates the horizontal and vertical variation of atmospheric refraction effects. It provides a fast and effective numerical solution for many long-distance EM propagation problems. Its wide application was due to the development of the split-step Fourier transform algorithm [12]. In [13], it was introduced as a means to calculate field intensity in anomalous propagation environments. Datasets used to train DL networks are generated by PETOOL [14], which is a one-way and two-way split-step PE program. PETOOL takes meteorological parameters as inputs and matrices of PL within the observation area as outputs. The one-way split-step solution is given by [14]

$$u(r+\Delta r,z)=\exp\left[ik_0\left(n^2-1\right)\frac{\Delta r}{2}\right]\cdot \mathcal{F}^{-1}\left\{\exp\left(-ik_0\sin^2\theta\frac{\Delta r}{2}\right)\mathcal{F}\{u(r,z)\}\right\} \quad (1)$$

where $u(r,z)$ denotes the field distribution, r is the distance, z is the altitude, Δr is the change in r, k_0 is the free-space wave number, n is the refractive index, θ is the propagation angle from the horizontal, and $\mathcal{F}$ indicates the Fourier transform. After obtaining $u(r,z)$, the propagation factor (PF) and the PL can be determined by [14]

$$PF=20\log|u(r,z)|+10\log(r)+10\log(\lambda) \quad (2)$$

$$PL=20\log\left(\frac{4\pi r}{\lambda}\right)-PF \quad (3)$$

$$=20\log(4\pi)+10\log(r)-30\log(\lambda)-20\log|u(r,z)|.$$

B. Supervised Learning and Linear Regression

Supervised learning (SL) is highly effective in handling prediction problems with known input data. SL models based on KNN, RF, and DNN can learn nonlinear functions for regression. The KNN method predicts the label of a new sample from the predefined number of training samples that are closest to it. RF is an ensemble algorithm that combines random decision trees to generate a prediction. A DNN generally consists of an input layer, one or more hidden layers, and an output layer. DNN maps the features of the input to a new feature space through layer-by-layer feature mapping, so as to learn a better feature expression for the output [15]. These models support multi-output problems where the output is a vector. Additionally, LR is an analytical method that uses linear statistical models to capture the relationship between independent and dependent variables.

In our simulations, the *LinearRegression*, *KNeighborsRegressor*, and *RandomForestRegressor* classes from the scikit-learn library are used to construct corresponding prediction models. The DNN model is implemented based on TensorFlow. The loss function in terms of mean squared error (MSE) can be calculated as

$$MSE=\frac{1}{N}\sum_{i=1}^{N}\|\boldsymbol{y}_i-\widehat{\boldsymbol{y}}_i\|_2^2 \quad (4)$$

where N denotes the total number of samples, $\boldsymbol{y}_i$ is the target vector, $\hat{\boldsymbol{y}}_i$ is the prediction vector, and $\|\cdot\|_2$ is the 2-norm.

C. Framework of DNN for PL Prediction

For model training, we construct two datasets, namely, the H_Data (1732500×509, each row records 500 PL values at a certain height, reflecting the variation of PL with distances) and the D_Data (2475000×354, each row records 345 PL values at a certain distance, reflecting the variation of PL with heights). The input features include environmental parameters and antenna parameters, which form a 1×9 vector. The target vector is a set of PL values with dimensions of 1×500 (or 1×345). The desired datasets are finally generated by simulating 1250 different environmental parameter settings and 198 different antenna parameter configurations and sampling the PL matrix calculated by PETOOL under each situation. Table I provides the ranges of input parameters. The reason why bands are limited to 3–20 GHz is that the waves at these frequencies are more susceptible to ducts and are important for future maritime wireless communications [4].

In order to explore the factors influencing prediction accuracy, we intentionally reserve a portion of the data with identical environmental parameters, which is not used in the model's training process. To ensure the generality of the network, the proportion of the training and testing sets is chosen as 70% and 30%. Furthermore, to enhance the convergence velocity and prediction accuracy of the DNN model, the datasets are scaled to a range of 0–1 and randomly shuffled.

To determine the structure of DNN, we explore the following parameter ranges: the number of hidden layers (1–10) and the number of neurons per hidden layer (10-1000). Through repeated testing and verification, it is found that the

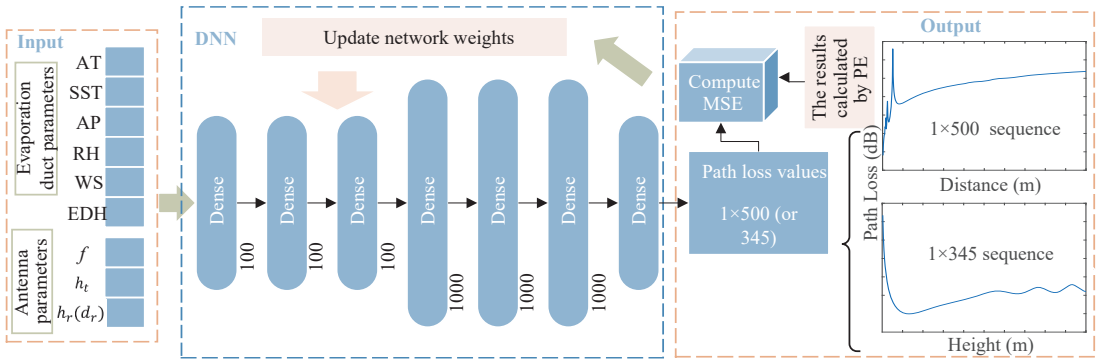

Fig. 1. The framework of DNN for PL prediction.

TABLE I
FEATURE PARAMETERS OF DATASETS.

Parameter	Range of values
Air temperature (AT)	21–25 °C
Sea surface temperature (SST)	14–16 °C
Air pressure (AP)	1011.9 / 1022.2 mbar
Relative humidity (RH)	40%–44%
Wind speed (WS)	9–11 m/s
Evaporation duct height (EDH)	From PETOOL
Frequency (f)	3–20 GHz
Transmitter height (h_t)	10–20 m
Receiver height (h_r) / Transmission distance (d_r)	Based on the sampling points

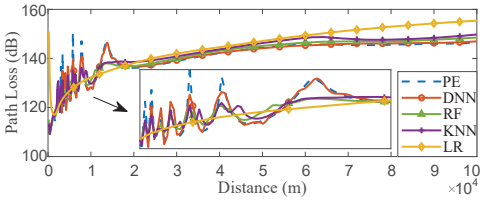

(a) H_Data, $h_r = 22$ m

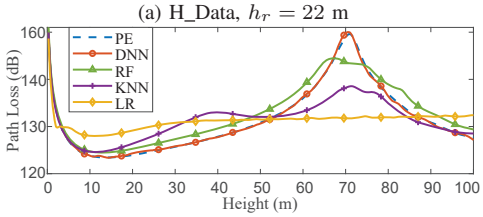

(b) D_Data, $d_r = 25$ m

Fig. 2. Prediction results at f=3 GHz and h_t=15 m.

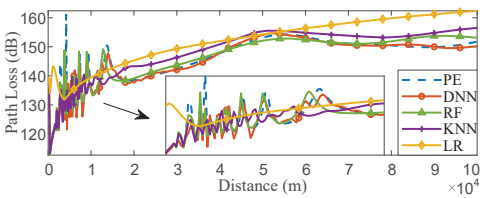

(a) H_Data, $h_r = 22$ m

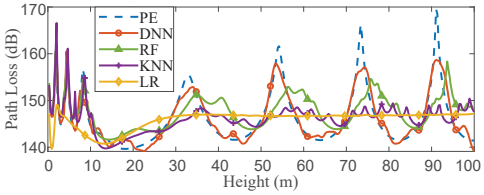

(b) D_Data, $d_r = 25$ m

Fig. 3. Prediction results at f=20 GHz and h_t=15 m.

superposition of the three-layer network is able to provide enough nonlinear expression ability without causing gradient problems and the 1000-dimension fully connected (FC) layers ensure that the network can learn enough features. Considering the balance between network performance and complexity, a DNN framework is proposed as shown in Fig. 1. Shallow 100-dimension FC layers are used for layer-by-layer feature mapping, and deep 1000-dimension FC layers extract rich features for complex function fitting. The ReLU activation function is chosen for its effectiveness. Two separate DNNs are trained for both datasets, differing only in the dimension of the output layer to accommodate the varying dimensions of the target vectors. Finally, prediction results are output through the linear activation by an FC layer with 500 (or 345) neurons.

We conduct training and performance tests on both datasets on Intel Core i9-12900K and NVIDIA GeForce RTX 3080. The number of epochs and batch size are set as 1000 and 32, respectively. The Adam optimizer with a learning rate of 0.001 is used. To further evaluate the networks' performance, mean absolute error (MAE) and normalized mean squared error (NMSE) are considered, as shown below

$$MAE = \frac{1}{N}\sum_{i=1}^{N} \|\boldsymbol{y}_i - \widehat{\boldsymbol{y}}_i\|_1 \tag{5}$$

$$NMSE = \frac{1}{N}\sum_{i=1}^{N} \frac{\|\boldsymbol{y}_i - \widehat{\boldsymbol{y}}_i\|_2^2}{\|\boldsymbol{y}_i\|_2^2} \tag{6}$$

where $\|\cdot\|_1$ is the 1-norm. The relative error, which is used to measure the deviation of prediction values, is calculated as

$$err = \frac{|y_{ij} - \widehat{y_{ij}}|}{y_{ij}} \times 100\% \tag{7}$$

where y_{ij} and $\widehat{y_{ij}}$ denote a value in the target and prediction vectors, respectively.

III. Results and Analysis

The comparison of different prediction schemes is shown in Fig. 2 and Fig. 3. The fact that DNN predicts accurately in both the peak and smooth regions indicates that DNN demonstrates superior fitting capabilities. In contrast, KNN and RF struggle to accurately predict the spikes and exhibit a fitting gap in the smooth region. LR can only track the trend of PL but lacks the ability to describe detailed changes. Notably, as the distance, height, or frequency increases, DNN demonstrates a more significant improvement in prediction accuracy compared to other models. Fig. 4 shows the prediction error distributions of DNN, KNN, RF, and LR on both datasets. The prediction errors of DNN are mainly concentrated in the range of 0–1 dB, while KNN, RF, and LR show concentrations in the range of 0–4 dB, 0–6 dB, and 0–10 dB, respectively.

The performance evaluations of different models are shown in Table II. On both datasets, the MAE, MSE, and NMSE values of results predicted by DNN are significantly lower

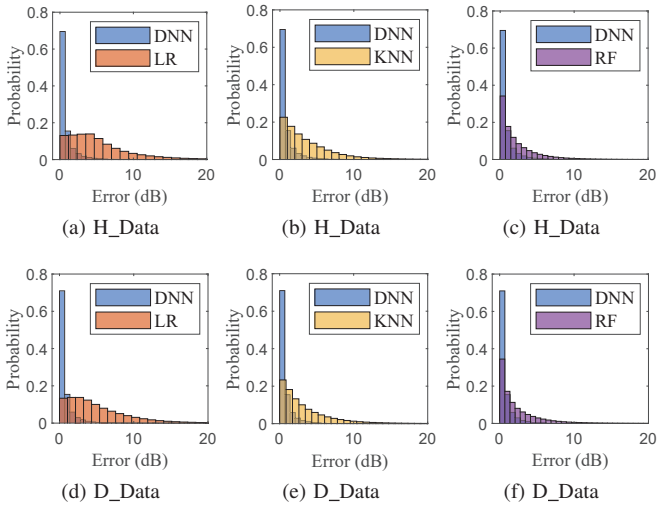

Fig. 4. Prediction errors of different models on both datasets.

TABLE II
ALGORITHM PERFORMANCE EVALUATION.

Evaluation indicator	H_Data				D_Data			
	LR	KNN	RF	**DNN**	LR	KNN	RF	**DNN**
MAE /dB	34.45	32.76	30.64	**26.17**	32.57	30.70	29.08	**24.06**
MSE /dB	44.66	41.57	38.23	**31.38**	42.46	39.44	36.81	**28.69**
NMSE /dB	-25.83	-28.87	-32.34	**-39.17**	-26.42	-28.91	-32.13	**-39.86**
$P_{err<5\%}$	0.755	0.861	0.947	**0.992**	0.780	0.874	0.945	**0.995**
$P_{err<1\%}$	0.165	0.316	0.528	**0.851**	0.182	0.367	0.538	**0.869**
Prediction time /μs	3	29	2	**23**	2	38	1	**18**

than those of KNN, RF, and LR. In the evaluation of prediction errors for DNN on both datasets, the proportion of predictions with errors below 5% ($P_{err<5\%}$) exceeds 99%, and the proportion of predictions with errors below 1% ($P_{err<1\%}$) exceeds 85%, which are significantly higher than those of KNN, RF, and LR. LR has a shorter running time because of its fewer network parameters, resulting in insufficient fitting ability. The long running time of KNN is attributed to the computation of distances between the test sample and all the training samples, and KNN is memory-intensive due to storing the training data. RF exhibits reasonable prediction accuracy and a shorter running time. However, because of the large and complex dataset, RF needs to store numerous decision trees, resulting in a large memory footprint in the order of gigabytes. DNN greatly improves prediction accuracy with acceptable time complexity while maintaining a small model size.

The influence of frequency, receiver height, and transmission distance on the PL prediction of DNN is compared, as shown in Fig. 5. On the H_Data, the prediction curves of different receiver heights closely match the PE results at low frequencies. However, as the frequency increases, the curve changes dramatically in peak regions, which affects the prediction accuracy of DNN in peak regions and smooth regions. We calculate the NMSE values of different frequencies respectively and find that the NMSE at 20 GHz is 5.93 dB higher than that at 3 GHz. On the D_Data, the comparison shows a similar phenomenon. The prediction accuracy at different transmission distances is similiar but slightly reduced

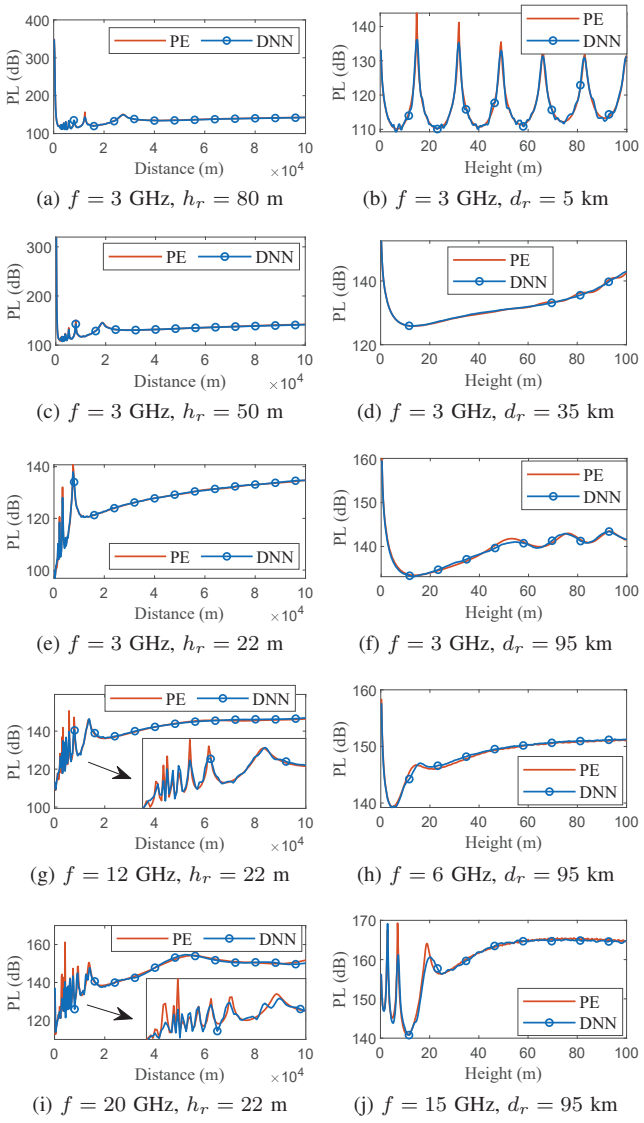

Fig. 5. Prediction results with the same environmental parameters, $h_t = 15$ m, and $EDH = 27$ m. Left: H_Data; Right: D_Data.

at higher frequencies (the NMSE at 20 GHz is 6.76 dB higher than that at 3 GHz).

IV. CONCLUSIONS

The proposed DNN scheme is effective and accurate for PL prediction in evaporation ducts. Including environment and antenna parameters in the model makes the input closer to actual situations. Numerical results have shown that DNN outperforms KNN, RF, and LR, achieving $P_{err<5\%}$ exceeding 99%. DNN has achieved a prominent improvement in prediction accuracy while maintaining a microsecond running time and a small model size. Furthermore, as the distance, height, or frequency increases, the accuracy improvement of DNN has become more remarkable than that of other models. The research on the prediction accuracy of DNN has revealed that receiver heights or transmission distances have no significant effect. However, the prediction accuracy of DNN may sightly decrease due to drastic changes in the peak region of the PL curve at higher frequencies.

REFERENCES

[1] C.-X. Wang, X. You, X. Gao, et al, "On the road to 6G: Visions, requirements, key technologies and testbeds," *IEEE Commun. Surveys Tuts.*, vol. 25, no. 2, pp. 905–974, Secondquarter 2023.

[2] B. Shang, Y. Yi, and L. Liu, "Computing over space-air-ground integrated networks: Challenges and opportunities," *IEEE Netw.*, vol. 35, no. 4, pp. 302–309, Aug. 2021.

[3] J. Wang, H. Zhou, Y. Li, Q. Sun, Y. Wu, S. Jin, T. Q. Quek, and C. Xu, "Wireless channel models for maritime communications," *IEEE Access*, vol. 6, pp. 68 070–68 088, Nov. 2018.

[4] E. Dinc, and O.B. Akan, "Beyond-line-of-sight communications with ducting layer," *IEEE Commun. Mag.*, vol. 52, no. 10, pp. 37–43, Oct. 2014.

[5] L. Yee Hui, F. Dong, and Y. S. Meng, "Near sea-surface mobile radiowave propagation at 5 GHz: Measurements and modeling," *Radioengineering*, vol. 23, no. 3, pp. 824–830, Sept. 2014.

[6] Q. Mao, F. Hu and, Q. Hao, "Deep learning for intelligent wireless networks: A comprehensive survey," *IEEE Commun. Surv. Tutor.*, vol. 20, no. 4, pp. 2595–2621, Jun. 2018.

[7] H. Zhang, T. Zhou, T. Xu, Y. Wang, and H. Hu, "Fnn-based prediction of wireless channel with atmospheric duct," in *Proc. IEEE ICC'21*. Montreal, QC, Canada, Jun. 2021, pp. 1–6.

[8] Z. Wei, J. Wu, B. Yin, D. Jia, and J. Xu, "Atmospheric duct propagation loss prediction based on time convolution network (TCN)," in *Proc. WCEEA'22*, Indianapolis, IN, USA, Oct. 2022, pp. 152–158.

[9] M. Dang, J. Wu, S. Cui, X. Guo, Y. Cao, H. Wei, and Z. Wu, "Multiscale decomposition prediction of propagation loss in oceanic tropospheric ducts," *Remote Sens.*, vol. 13, no. 6, Mar. 2021.

[10] H. Ji, B. Yin, J. Zhang, Y. Zhang, Q. Li, C. Hou, "Multiscale decomposition prediction of propagation loss for EM waves in marine evaporation duct using deep learning," *J. Mar. Sci. Eng.*, vol. 11, no. 1, Jan. 2023.

[11] S. Wang, K. Yang, Y. Shi, F. Yang, H. Zhang, and Y. Ma, "Prediction of over-the-horizon electromagnetic wave propagation in evaporation ducts based on the Gated Recurrent Unit network model," *IEEE Trans. Antennas Propag.*, vol. 71, no. 4, pp. 3485–3496, Apr. 2023.

[12] R. H. Hardin, and F.D. Tappert, "Applications of the split-step Fourier method to the numerical solution of nonlinear and variable coefficient wave equations," *SIAM Rev.* vol. 15, pp. 423, Jan. 1973.

[13] H. W. Ko, J. W. Sari, and J. P. Skura, "Anomalous microwave propagation through atmospheric ducts," *Johns Hopkins APL Tech. Dig.*, vol. 4, no. 1, pp. 12–26, Mar. 1983.

[14] O. Ozgun, G. Apaydin, M. Kuzuoglu, and L. Sevgi, "Petool: Matlab-based one-way and two-way split-step parabolic equation tool for radiowave propagation over variable terrain," *Comput. Phys. Commun.*,vol. 182, no. 12, pp. 2638–2654, Jul. 2011.

[15] V. Sze, Y. -H. Chen, T. -J. Yang, and J.S. Emer, "Efficient processing of deep neural networks: A tutorial and survey," *Proceedings of the IEEE*, vol. 105, no. 12, pp. 2295–2329, Dec. 2017.